

PM/96-08
 THES-TP 96/02
 February 1996

Residual New Physics Effects in e^+e^- and $\gamma\gamma$ Collisions at NLC ¹

G.J. Gounaris^a, J.Layssac^b, J.E. Paschalis^a, F.M. Renard^b
 and N.D. Vlachos^a

^aDepartment of Theoretical Physics, University of Thessaloniki,
 Gr-54006, Thessaloniki, Greece,

^bPhysique Mathématique et Théorique, CNRS-URA 768,
 Université de Montpellier II, F-34095 Montpellier Cedex 5.

Contribution to the NLC workshop

Abstract

We report on a set of studies concerning the description of New Physics (NP) effects characterized by a scale much higher than the electroweak scale. We concentrate on the residual effects described by an effective lagrangian involving only bosonic fields and restrict to the case that the Higgs field is described linearly, so that the Higgs particle exists. It has already been emphasized that this lagrangian may be represented by eight $dim = 6$ operators; namely the blind CP-conserving operators \mathcal{O}_W , $\mathcal{O}_{B\Phi}$, $\mathcal{O}_{W\Phi}$, \mathcal{O}_{UB} , \mathcal{O}_{UW} , the "superblind" \mathcal{O}_{Φ_2} and the two CP-violating ones $\overline{\mathcal{O}}_{UB}$ and $\overline{\mathcal{O}}_{UW}$. To each operator and for any given value of its coupling, we associate an unambiguous NP scale determined by the energy where unitarity is saturated. Our study of the possible NP tests realizable at a future linear e^+e^- collider concentrates on ($e^+e^- \rightarrow HZ$, $H\gamma$), and on $\gamma\gamma$ collisions producing boson pairs ($\gamma\gamma \rightarrow W^+W^-$, ZZ , $Z\gamma$, $\gamma\gamma$, HH), or a single Higgs ($\gamma\gamma \rightarrow H$). The sensitivities to the various operators involved in the effective lagrangian are estimated. We find that the testable NP scales vary from a few tens of TeV in the boson pair processes, up to 65 TeV in single H production. Ways to disentangle the various operators are also proposed. In this respect a comparison of the NP effects in the various boson pair processes, like *e.g.* a comparison of $e^+e^- \rightarrow HZ$ versus $e^+e^- \rightarrow H\gamma$, should be very fruitful. This is applied also to the study of the Higgs branching ratios, and especially the ratio $\Gamma(H \rightarrow \gamma\gamma)/\Gamma(H \rightarrow \gamma Z)$.

¹Partially supported by the EC contract CHRX-CT94-0579.

1 Introduction

The search for manifestations of New Physics (NP) is an important part of the program of future high energy colliders. If it happens that all new particles are too heavy to be directly produced at these colliders, then the only way NP could manifest itself, is through residual interactions affecting the particles already present in SM. The possibility for such residual NP effects involving the interactions of the gauge bosons with the leptons and to some extent the light quarks, has already been essentially excluded by LEP1. Thus, the self-interactions among the gauge and Higgs bosons and possibly also the heavy quarks constitute the most probable space for some NP. On the other hand the scalar sector is the most mysterious part of the Standard Model (SM) of the electroweak interactions and is the favorite place for generating New Physics (NP) manifestations.

High energy e^+e^- linear colliders will offer many possibilities to test the sector of the gauge boson and Higgs interactions with a high accuracy, firstly in e^+e^- collisions and secondly through $\gamma\gamma$ collisions. The most famous process is $e^+e^- \rightarrow W^+W^-$. This has been carefully studied and it has been shown that indeed the 3-gauge boson vertices γW^+W^- and ZW^+W^- can be very accurately constrained through it. If the Higgs boson is not too heavy further processes to consider are $e^-e^+ \rightarrow ZH$, γH . In SM, the process $e^-e^+ \rightarrow Z \rightarrow ZH$ is allowed at tree level, while $e^-e^+ \rightarrow \gamma H$ is only possible at 1-loop level and is therefore a dedicated place to look for anomalous Higgs-gauge boson interactions.

A new facility offered by high energy linear e^+e^- colliders is the realization of $\gamma\gamma$ collisions with intense high energy photon beams through the laser backscattering method. This will give access to a new kind of processes namely boson-boson scattering. Five boson pair production processes are thus accessible, $\gamma\gamma \rightarrow W^+W^-$, ZZ , $Z\gamma$, $\gamma\gamma$ and HH . Such processes are very interesting, since they are sensitive not only to the 3-gauge boson vertices, but also to 4-gauge boson as well as to Higgs couplings. In addition, provided the Higgs particle will be accessible at the future colliders, the $\gamma\gamma$ fusion into a single Higgs boson will give direct access to the study of this particle and thus test the scalar sector in a much deeper way, particularly because the standard contribution to $\gamma\gamma \rightarrow H$ only occurs at 1-loop. With the high luminosities expected at linear e^+e^- colliders, thousands of Higgs bosons should be produced. The sensitivity to anomalous $H\gamma\gamma$ couplings is therefore very strong.

Below we summarize the studies in [1, 2, 3] and show that they provide very sensitive tests of the various possible forms of² NP.

Assuming that the NP scale Λ_{NP} is sufficiently large, the effective NP Lagrangian should be satisfactorily described in terms of $dim = 6$ bosonic operators only. There exist only seven $SU(2) \times U(1)$ gauge invariant such operators called "blind", which are not strongly constrained by existing LEP1 experiments. Three of them

$$\mathcal{O}_W = \frac{1}{3!} \left(\vec{W}_\mu{}^\nu \times \vec{W}_\nu{}^\lambda \right) \cdot \vec{W}_\lambda{}^\mu, \quad (1)$$

$$\mathcal{O}_{W\Phi} = i (D_\mu \Phi)^\dagger \vec{\tau} \cdot \vec{W}^{\mu\nu} (D_\nu \Phi) \quad , \quad \mathcal{O}_{B\Phi} = i (D_\mu \Phi)^\dagger B^{\mu\nu} (D_\nu \Phi) \quad (2)$$

²Because of lack of space, the extensive literature on the subject is not given explicitly and can be found in [1, 2, 3].

induce anomalous triple gauge boson couplings, while the remaining four

$$\mathcal{O}_{UW} = \frac{1}{v^2} (\Phi^\dagger \Phi - \frac{v^2}{2}) \vec{W}^{\mu\nu} \cdot \vec{W}_{\mu\nu} \quad , \quad \mathcal{O}_{UB} = \frac{4}{v^2} (\Phi^\dagger \Phi - \frac{v^2}{2}) B^{\mu\nu} B_{\mu\nu} \quad , \quad (3)$$

$$\overline{\mathcal{O}}_{UW} = \frac{1}{v^2} (\Phi^\dagger \Phi) \vec{W}^{\mu\nu} \cdot \vec{\widetilde{W}}_{\mu\nu} \quad , \quad \overline{\mathcal{O}}_{UB} = \frac{4}{v^2} (\Phi^\dagger \Phi) B^{\mu\nu} \widetilde{B}_{\mu\nu} \quad (4)$$

create anomalous CP conserving and CP violating Higgs couplings.

In addition, the "superblind" operator

$$\mathcal{O}_{\Phi 2} = 4 \partial_\mu (\Phi^\dagger \Phi) \partial^\mu (\Phi^\dagger \Phi) \quad , \quad (5)$$

which is insensitive to LEP1 physics even at the 1-loop level, induces a wave function renormalization to the Higgs field that may be observable in $e^- e^+ \rightarrow ZH$.

The effective Lagrangian describing the NP induced by these operators is given by

$$\begin{aligned} \mathcal{L}_{NP} = & \lambda_W \frac{g}{M_W^2} \mathcal{O}_W + \frac{f_B g'}{2M_W^2} \mathcal{O}_{B\Phi} + \frac{f_W g}{2M_W^2} \mathcal{O}_{W\Phi} + \\ & d \mathcal{O}_{UW} + \frac{d_B}{4} \mathcal{O}_{UB} + \overline{d} \overline{\mathcal{O}}_{UW} + \frac{\overline{d}_B}{4} \overline{\mathcal{O}}_{UB} + \frac{f_{\Phi 2}}{v^2} \mathcal{O}_{\Phi 2} \quad , \end{aligned} \quad (6)$$

which defines the various couplings. Studying unitarity, we have established relations between these coupling constants and the corresponding NP scales Λ_{NP} (defined as the energy value at which unitarity is saturated). This allows us to express the observability limits directly in terms of Λ_{NP} .

We now study how the aforementioned processes accessible at NLC react to each of these operators and what is the observability limit for the associated NP scale. We also give ways to disentangle the effects of the various operators.

2 Analysis of $e^- e^+ \rightarrow Z_{(f\bar{f})} H$ and $e^- e^+ \rightarrow \gamma H$.

Using the NP lagrangian given by (6), we have computed in [1] the helicity amplitude for $e^- e^+ \rightarrow ZH$. They depend on the SM couplings and on the combinations of NP couplings $d_{\gamma Z} = s_W c_W (d - d_B)$, $d_{ZZ} = d c_W^2 + d_B s_W^2$, $d_{\gamma\gamma} = d s_W^2 + d_B c_W^2$, as well as the corresponding CP-violating ones for \overline{d} , \overline{d}_B defined in (6).

The corresponding total cross section as a function of the $e^- e^+$ energy is shown in Fig.1 assuming $m_H = 80 GeV$. In this figure, we present results for various values of the d and d_B couplings, indicating also the NP scale they correspond to. Identical results are of course also obtained for the same values of the CP-violating couplings \overline{d} and \overline{d}_B respectively. The HZ angular distribution depends on $f_{\Phi 2}$ through the Higgs field renormalization factor Z_H , while its dependence on \mathcal{O}_{UW} and \mathcal{O}_{UB} is mainly given by the combination d_{ZZ} (see Fig.2).

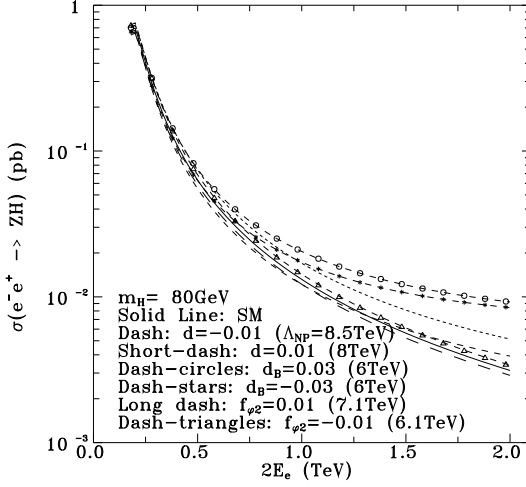


Fig 1

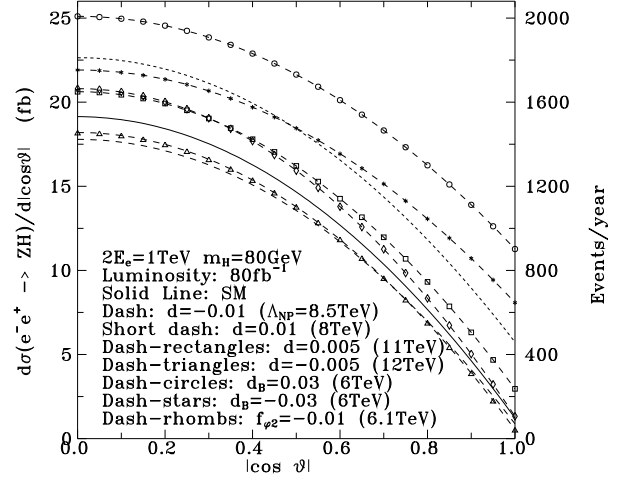


Fig 2

Thus at 1 TeV , with 80 fb^{-1} per year, the SM rate gives one thousand events per year. One can then expect a measurement of the cross section with a 3% accuracy. The implied sensitivities to the various couplings are $|f_{\phi 2}| \simeq 0.004$, $|d| \simeq 0.005$ and $|d_B| \simeq 0.015$, corresponding to NP scales of 10, 11 and 9 TeV respectively; compare Fig.1 and Fig.2. Moreover, with such a number of events, informations from the fermionic decay distribution of the Z can be used in order to disentangle the various d -type couplings.

We then compute the Z density matrix in the helicity basis and, assuming that the decay $Z \rightarrow f\bar{f}$ is standard, the angular distribution for the $f\bar{f}$ system in the Z rest frame. In [1] it was shown that the ϕ_f azimuthal distribution allows to define four asymmetries A_{13} , A_{12} , A_{14} , A_8 , respectively associated to the $\sin 2\phi_f$, $\cos 2\phi_f$, $\sin \phi_f$, $\cos \phi_f$ dependences. The remarkable features are that A_{14} , A_{12} are mainly sensitive on the combination $d_{\gamma Z}$ and on its CP -violating partner $\bar{d}_{\gamma Z}$. Thus, the illustrations made for $d, (\bar{d})$ apply also to $-d_B, (-\bar{d}_B)$. They are shown in Figs.3,4. These asymmetries depend on the flavour of the fermion f to which Z decays and are mostly interesting for the $Z \rightarrow b\bar{b}$ case. The asymmetry A_{13} shown in Fig.5 does not depend on the type of the fermion f and it is sensitive to the CP -violating combination \bar{d}_{ZZ} . Thus, sensitivities to this coupling at the percent level should be possible using this asymmetry. Note that in this case the sensitivities to \bar{d}_B and \bar{d} are related by $\bar{d}_B \simeq \bar{d} c_W^2 / s_W^2$. Finally the asymmetry A_8 shown in Fig.6, is also mainly sensitive to d_{ZZ} and independent of the flavour of the f fermion. Consequently, the differential cross section for $e^-e^+ \rightarrow ZH$, together with the above asymmetries, provide considerable information for disentangling the aforementioned five relevant anomalous couplings at the percent level. It follows that NP scales of the order of a few TeV could be searched for this way.

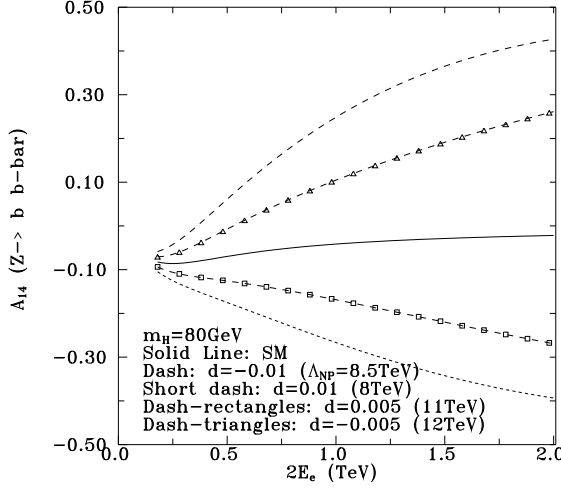


Fig 3

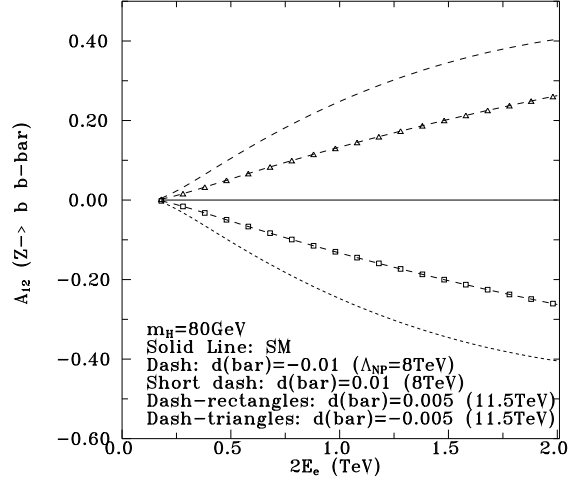


Fig 4

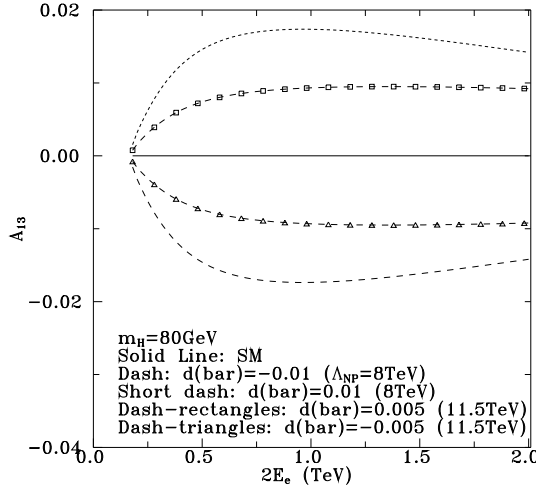


Fig 5

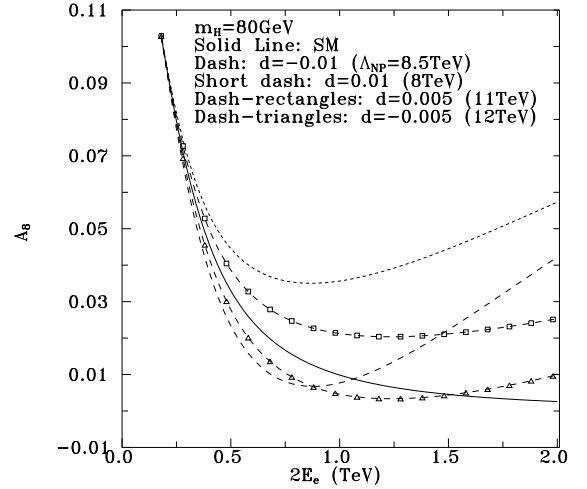


Fig 6

We next turn to the process $e^-e^+ \rightarrow \gamma H$. In this case [1] the NP contribution is added to the 1-loop SM contribution. We have again neglected tree-level contributions quadratic in the anomalous couplings, and also 1-loop contributions linear in the anomalous couplings. This implies that no contribution from $\mathcal{O}_{\Phi 2}$ should be included. At SM the cross section is unobservably small, but it is very sensitive to the four NP interactions and provides informations on combinations of couplings that are different from those appearing in $e^+e^- \rightarrow ZH$. The differential cross section could become observable if non negligible anomalous interactions occur. For a 1 TeV NLC, Fig.7a,b show the sensitivity to $|d| \simeq 0.005$ and $|d_B| \simeq 0.0025$ corresponding to NP scales of 11 TeV and 22 TeV respectively. In these figures we have used for illustration $m_H = 80 \text{ GeV}$, but of course similar results would have been expected for any $m_H \ll 1 \text{ TeV}$.

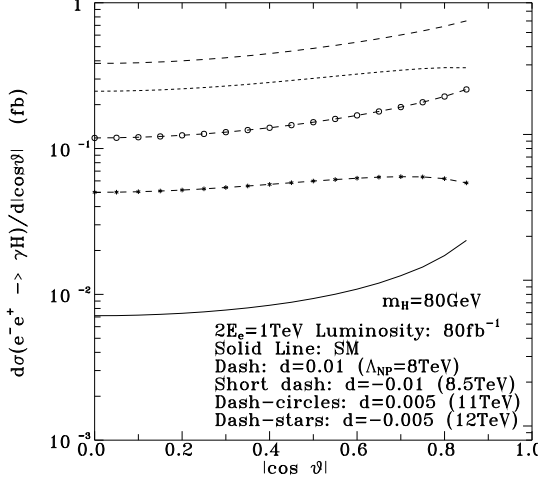


Fig 7a

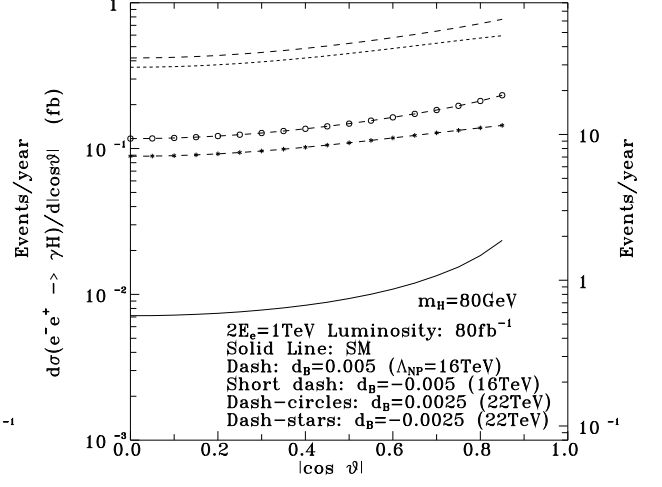


Fig 7b

3 Boson Pair Production Processes in $\gamma\gamma$ Collisions

The boson pair production processes that we consider here [3] are $\gamma\gamma \rightarrow W^+W^-$, $\gamma\gamma \rightarrow ZZ$, $\gamma\gamma \rightarrow HH$ and also $\gamma\gamma \rightarrow \gamma Z$, $\gamma\gamma \rightarrow \gamma\gamma$.

An efficient way of doing this is by looking at the transverse-momentum distribution of one of the final bosons B_3 and B_4 and cutting-off the small p_T values. It is given by

$$\frac{d\sigma}{dp_T dy} = \frac{y p_T}{8\pi s_{\gamma\gamma} |\Delta|} \int_{\frac{\tau}{x_{max}}}^{x_{max}} dx f_{\gamma/e}^{laser}(x) f_{\gamma/e}^{laser}\left(\frac{\tau}{x}\right) \Sigma |F(\gamma\gamma \rightarrow B_3 B_4)|^2, \quad (7)$$

where $y \equiv \sqrt{\tau} \equiv \sqrt{\frac{s_{\gamma\gamma}}{s_{ee}}}$, $|\Delta| = \frac{1}{2} \sqrt{s_{\gamma\gamma}(s_{\gamma\gamma} - 4(p_T^2 + m^2))}$, $p_T^2 < \frac{s_{\gamma\gamma}}{4} - m^2$ and $F(\gamma\gamma \rightarrow B_3 B_4)$ is the invariant amplitude of the subprocess given in [3]. $f_{\gamma/e}^{laser}(x)$ is the photon flux distribution.

The $\frac{d\sigma}{dp_T}$ distribution provides a very useful way for searching for NP, since it not only takes care of the events lost along the beam pipe, but also because its measurement does not require full reconstruction of both final bosons, at it would be the case for $\frac{d\sigma}{dy}$. For the illustrations below we choose $p_T > p_T^{min} = 0.1 TeV/c$. The correspondingly expected number of events per year is obtained by multiplying the above distribution by the integrated e^+e^- annual luminosity $\bar{\mathcal{L}}_{ee}$ taken to be $20, 80, 320 fb^{-1} year^{-1}$ for a 0.5, 1. or 2.TeV collider respectively.

We now summarize the properties of each of the five channels and the way they react to the residual NP lagrangian. SM contributes to $\gamma\gamma \rightarrow W^+W^-$ at tree level (through W exchange diagrams in the t, u channels involving the γWW vertex and the $\gamma\gamma WW$ contact term), and at the 1-loop level to the other processes. So the search for NP effects can be done by precision measurements in the W^+W^- channel and by looking for an observable enhancement in the other channels, see Fig.8-11. The results presented below are obtained in ref.[3] using asymptotic expressions for the anomalous parts of the

amplitudes in $\gamma\gamma \rightarrow W^+W^-$, $\gamma\gamma \rightarrow ZZ$, $\gamma\gamma \rightarrow \gamma Z$, $\gamma\gamma \rightarrow \gamma\gamma$, but exact expressions in the $\gamma\gamma \rightarrow HH$ case.

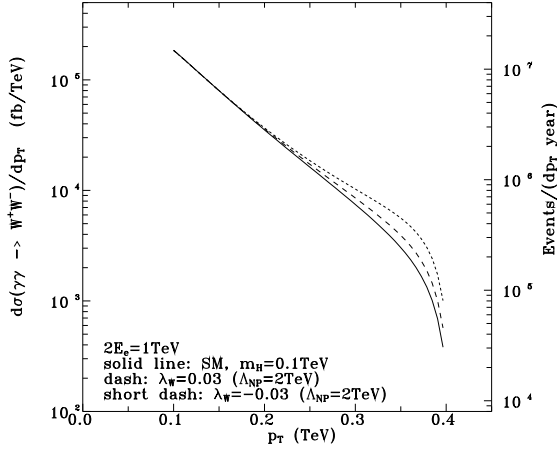


Fig 8

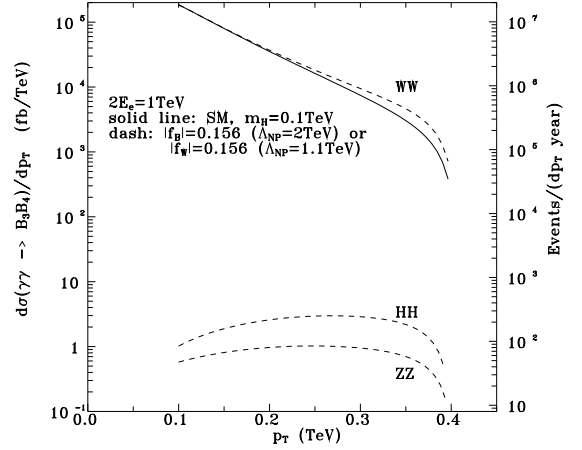


Fig 9

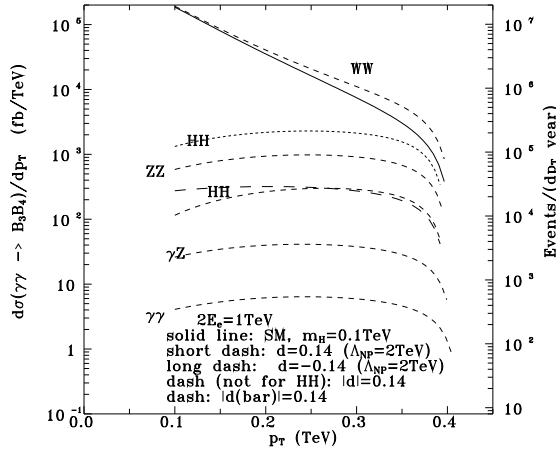


Fig 10

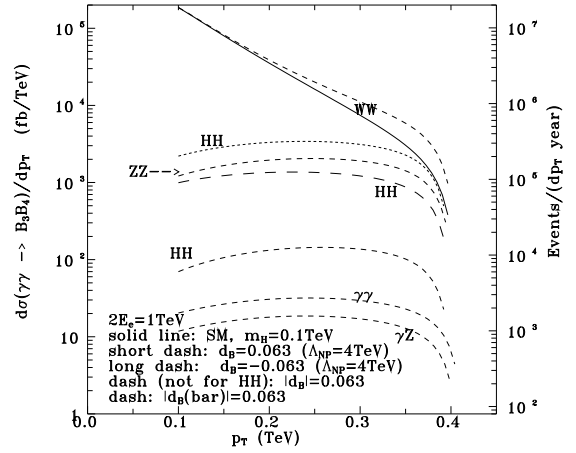


Fig 11

Table 1 shows how each operator contributes to the various channels, and one observes that the disentangling is possible between three groups of operators. In the \mathcal{O}_W case W^+W^- are produced in (TT) states whereas in the $\mathcal{O}_{B\Phi}$ and $\mathcal{O}_{W\Phi}$ cases it is mainly (LL). There is no way to distinguish the contributions of $\mathcal{O}_{B\Phi}$ from that of $\mathcal{O}_{W\Phi}$ in $\gamma\gamma$ collisions. The discrimination between these two operators requires the use of other processes, like $e^+e^- \rightarrow W^+W^-$. The disentangling of \mathcal{O}_{UW} from \mathcal{O}_{UB} can then be done by looking at the ratios of the ZZ and WW cross sections. Notice that the linear terms of the WW and ZZ amplitudes for \mathcal{O}_{UB} may be obtained from the corresponding terms for \mathcal{O}_{UW} by multiplying by the factor c_W^2/s_W^2 .

There is no way to separate the CP-conserving from the CP-violating terms in these spectra. More detailed spin analyses are required, like *e.g.* the search for imaginary parts in final W or Z spin density matrices observable through the decay distributions or the measurement of asymmetries associated to linear polarizations of the photon beams.

	SM	\mathcal{O}_W	$\mathcal{O}_{W\Phi}$	$\mathcal{O}_{B\Phi}$	\mathcal{O}_{UW}	\mathcal{O}_{UB}	$\overline{\mathcal{O}}_{UW}$	$\overline{\mathcal{O}}_{UB}$
$\gamma\gamma \rightarrow WW$	TT	TT	LL	LL	LL	LL	LL	LL
$\gamma\gamma \rightarrow ZZ$			TT	TT	LL	LL	LL	LL
$\gamma\gamma \rightarrow HH$			X	X	X	X	X	X
$\gamma\gamma \rightarrow \gamma Z$					TT	TT	TT	TT
$\gamma\gamma \rightarrow \gamma\gamma$					TT	TT	TT	TT

Table 1: Contributions from the various operators

Table 2 summarizes the observability limits expected for each operator on the basis of W^+W^- production alone. To derive them we assume that a 5% departure of the W^+W^- cross section in the high p_T range from the SM prediction, will be observable. These observability limits on the anomalous couplings give essentially lower bounds for the couplings to be measurable, that correspond to upper limits for observable Λ_{NP} .

	\mathcal{O}_W		\mathcal{O}_{UW} or $\overline{\mathcal{O}}_{UW}$		\mathcal{O}_{UB} or $\overline{\mathcal{O}}_{UB}$		$\mathcal{O}_{B\Phi}$ or $\mathcal{O}_{W\Phi}$	
$2E_e(\text{TeV})$	$ \lambda_W $	Λ_{NP}	$ d $ or $ \overline{d} $	Λ_{NP}	$ d_B $ or $ \overline{d}_B $	Λ_{NP}	$ f_B $ or $ f_W $	Λ_{NP}
0.5	0.04	1.7	0.1	2.4	0.04	4.9	0.2	1.8, 1
1	0.01	3.5	0.04	4	0.015	9	0.05	3.5, 2
2	0.003	6.4	0.015	7	0.005	16	0.015	6.5, 3.6

Table 2: Observability limits based on the W^+W^- channel to the anomalous couplings and the related NP scales Λ_{NP} (TeV).

At 2 TeV, in the case of the operators \mathcal{O}_{UB} , \mathcal{O}_{UW} , $\overline{\mathcal{O}}_{UB}$, $\overline{\mathcal{O}}_{UW}$ slightly better limits could in principle be obtained by using the $\gamma\gamma \rightarrow ZZ$ process. Demanding for example that the NP contribution to this process reaches the level of the SM result for $\gamma\gamma \rightarrow ZZ$, we can decrease the limiting value for the couplings $|d|$ (or $|\overline{d}|$) and $|d_B|$ (or $|\overline{d}_B|$) down to 0.01 and 0.003 respectively. This means that a 2 TeV collider is sensitive to NP scales up to 20 TeV. A more precise analysis using realistic uncertainties for the detection of the ZZ channel and taking into account the interference between the SM and the NP contributions, could probably improve these limits. This needs more work.

4 The fusion $\gamma\gamma \rightarrow H$

The cross section for $\gamma\gamma \rightarrow H$ is given by [2]

$$\sigma = \mathcal{L}_{\gamma\gamma}(\tau_H) \left(\frac{8\pi^2}{m_H} \right) \frac{\Gamma(H \rightarrow \gamma\gamma)}{s_{ee}} \quad , \quad (8)$$

where the luminosity function $\mathcal{L}_{\gamma\gamma}(\tau_H)$ for $\tau_H = m_H^2/s_{ee}$ is explicitly given in terms of the $f_{\gamma/e}^{laser}$ distribution in [2, 3]. Essentially $\mathcal{L}_{\gamma\gamma}$ is close to the e^+e^- linear collider luminosity \mathcal{L}_{ee} up to $\tau_{max} = (0.82)^2$.

The $H \rightarrow \gamma\gamma$ decay width is computed in terms of the one-loop SM contribution and tree level NP ones [2] obtained from the Lagrangian given in eqs. (8):

$$\Gamma(H \rightarrow \gamma\gamma) = \frac{\sqrt{2}G_F}{16\pi} m_H^3 \left(\left| \frac{\alpha}{4\pi} \left(\frac{4}{3}F_t + F_W \right) - 2ds_W^2 - 2d_Bc_W^2 \right|^2 + 4|\bar{d}s_W^2 + \bar{d}_Bc_W^2|^2 \right), \quad (9)$$

where the standard top (F_t) and W (F_W) contributions are explicitly given in [2].

The resulting rate is shown in Fig.12-13 for a 1 TeV collider. The number of events indicated in these figures corresponds to an e^+e^- luminosity of 80 fb^{-1} . Strong interference effects may appear (depending on the Higgs mass) between the SM and the CP-conserving NP contributions; (compare Fig.12). But in the case of CP-violating contributions (Fig.13) there are never such interferences. In the figures we have only illustrated the cases of \mathcal{O}_{UW} and $\overline{\mathcal{O}}_{UW}$. The corresponding results for \mathcal{O}_{UB} and $\overline{\mathcal{O}}_{UB}$ can be deduced according to eq(9) from Fig.12-13, by the replacement $d[\bar{d}] \rightarrow c_W^2/s_W^2 d_B[\bar{d}_B]$. So the sensitivity to these last two operators is enhanced by more than a factor 3 in the cross section.

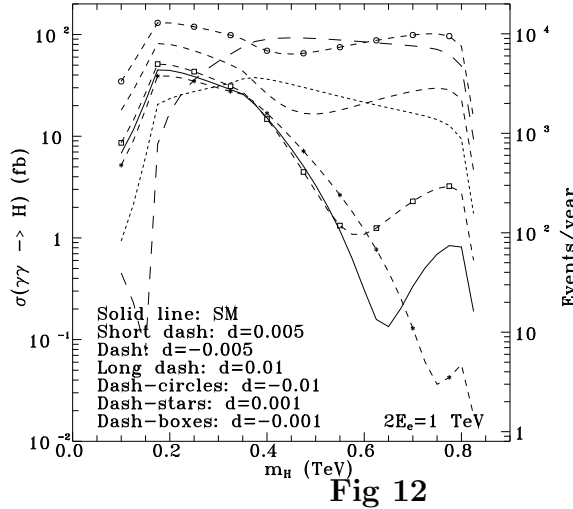


Fig 12

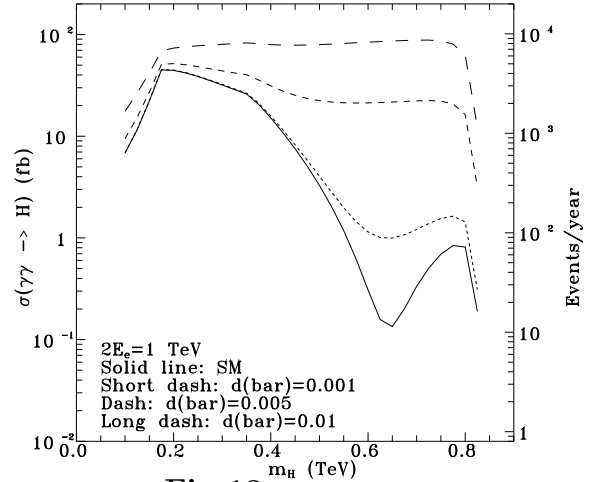


Fig 13

With the aforementioned designed luminosities, one gets a few thousands of Higgs bosons produced in the light or intermediate mass range. Assuming conservatively an experimental detection accuracy of about 10% on the production rate, one still gets an observability limit of the order of 10^{-3} , $4 \cdot 10^{-3}$, $3 \cdot 10^{-4}$, 10^{-3} for d , \bar{d} , d_B and \bar{d}_B respectively. The corresponding constraints on the NP scale are 26, 13, 65, 36 TeV respectively.

5 NP searches through ratios of Higgs decay widths

In this Section we show that independently of the Higgs production mechanism, the study of the Higgs branching ratios can be very fruitful for NP searches and for disentangling contributions from the various operators.

The expression of the $H \rightarrow \gamma\gamma$ width has been given in (9). Correspondingly, the $H \rightarrow \gamma Z$ width is also expressed in terms of a 1-loop SM contribution and of the NP contributions from the four operators. The $H \rightarrow W^+W^-, ZZ$ widths are explicitly given in [2]. They receive a tree level SM contribution which interferes with the ones from the CP-conserving operators $\mathcal{O}_{UB}, \mathcal{O}_{UW}$. Finally we note that the $H \rightarrow b\bar{b}$ decay width is purely standard and particularly important if $m_H < 140\text{GeV}$. In Figs. 14a,b the ratios $\Gamma(H \rightarrow \gamma\gamma)/\Gamma(H \rightarrow b\bar{b})$ and $\Gamma(H \rightarrow \gamma Z)/\Gamma(H \rightarrow b\bar{b})$ are plotted versus m_H for a given value of d or \bar{d} . The case of d_B or \bar{d}_B can be obtained by the respective replacements $d \rightarrow d_B c_W^2/s_W^2$ for the $\gamma\gamma$ amplitude and of $d \rightarrow d_B$ for the γZ one. The m_H and d dependences of the $\gamma\gamma/b\bar{b}$ ratio are obviously similar to the ones of the production cross section $\sigma(\gamma\gamma \rightarrow H)$. The ratios $\gamma Z/b\bar{b}$ and $\gamma\gamma/\gamma Z$ have independent features that may help disentangling the various couplings. They can also be seen from the ratio shown in Fig.14c.

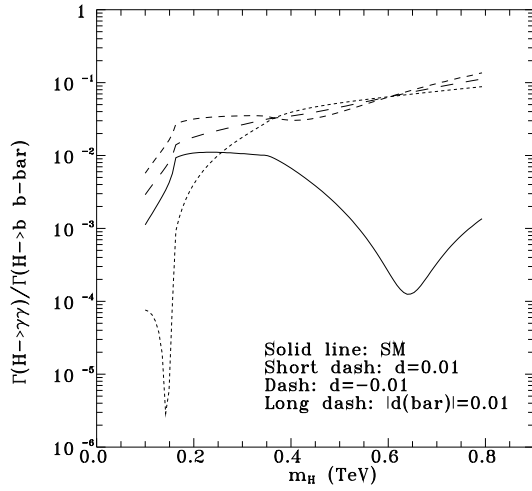


Fig 14a

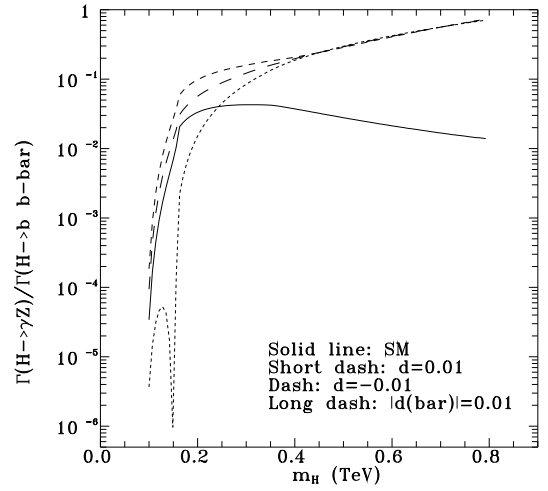


Fig 14b

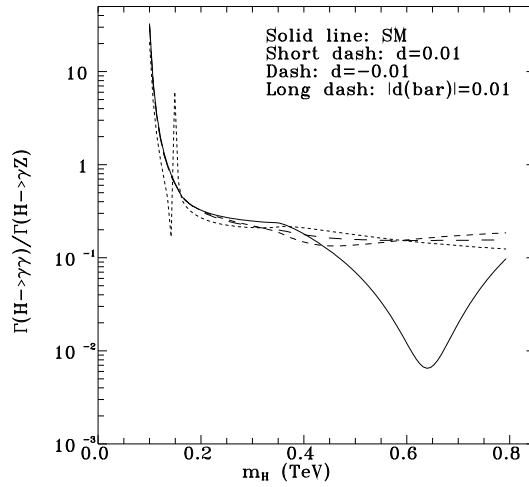


Fig14c

The sensitivity of the $WW/b\bar{b}$ and $ZZ/b\bar{b}$ ratios is much weaker as expected from the occurrence of tree level SM contributions. Because of this these ratios are only useful for $|d| \gtrsim 0.1$. The ratios $\gamma\gamma/WW$ and $\gamma\gamma/ZZ$ are shown in Figs.14d,e and present the same features as the ratio $\gamma\gamma/b\bar{b}$. They can however be useful in the range of m_H where the WW, ZZ modes are dominant.

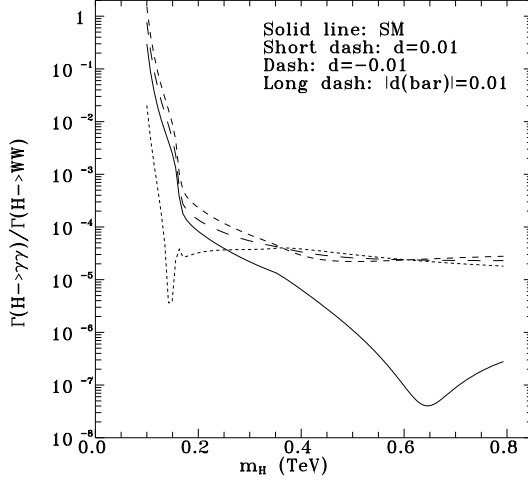


Fig 14d

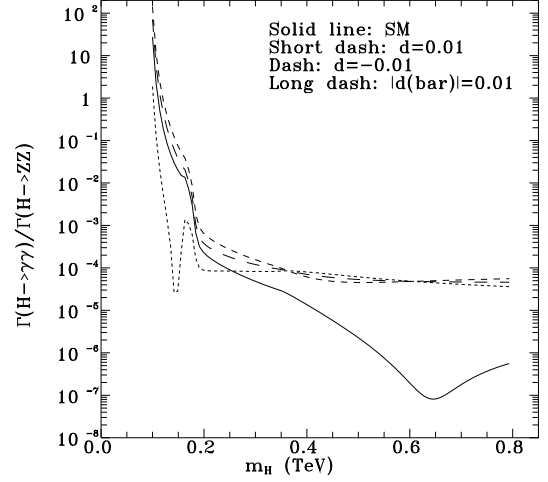


Fig 14e

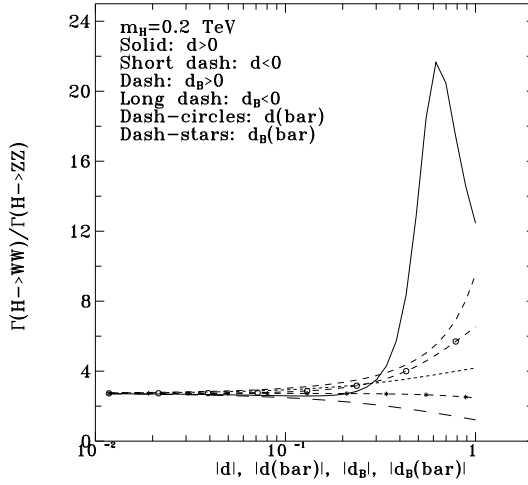


Fig 15a

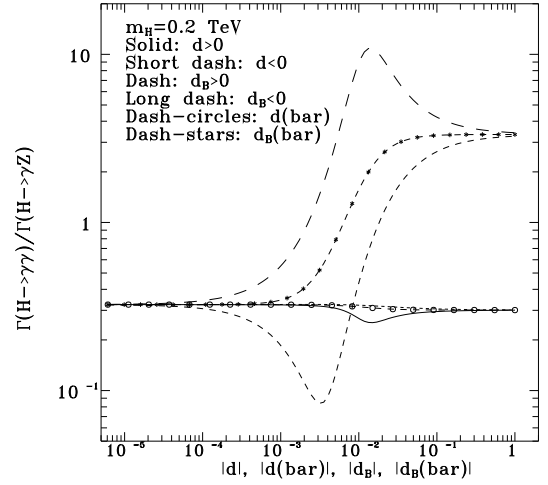


Fig 15b

Finally we discuss the ratios WW/ZZ and $\gamma\gamma/\gamma Z$ for a given value of m_H (chosen as 0.2TeV in the illustrations made in Fig.15a,b), versus the coupling constant values of the four operators. This shows very explicitly how these ratios can be used for disentangling the various operators. They have to be taken in a complementary way to the $\sigma(\gamma\gamma \rightarrow H)$ measurement. As in the $WW/b\bar{b}$ case, the WW/ZZ ratio is only useful for $|d| \gtrsim 0.1$, while $\gamma\gamma/\gamma Z$ ratio allows for disentangling d values down to 10^{-3} or even less. The corresponding sensitivity limit for d_B, \bar{d}_B should then be lying at the level of a few times 10^{-4} .

6 Final discussion

We have concentrated our analysis on the residual NP effects described by seven blind and one superblind $dim = 6$ $SU(2) \times U(1)$ gauge invariant operators \mathcal{O}_W , $\mathcal{O}_{B\Phi}$, $\mathcal{O}_{W\Phi}$, \mathcal{O}_{UB} , \mathcal{O}_{UW} , $\overline{\mathcal{O}}_{UB}$, $\overline{\mathcal{O}}_{UW}$, $\mathcal{O}_{\Phi 2}$. The first three ones should be essentially studied in the process $e^+e^- \rightarrow W^+W^-$ but they also contribute to $\gamma\gamma \rightarrow WW$. The five other ones only affect the Higgs couplings to themselves and to gauge bosons, and their effects have been considered in all processes in which a Higgs can be exchanged or produced.

We started with the Higgs production process $e^-e^+ \rightarrow ZH$. We have analyzed the angular distributions for HZ as well as the four azimuthal asymmetries in $Z \rightarrow f\bar{f}$ decays associated to the $\cos\phi_f$, $\sin\phi_f$, $\sin 2\phi_f$ and $\cos 2\phi_f$ distributions controlled by the Z spin density matrix elements. The disentangling of the five relevant operators should be achievable down to the percent level for the NP couplings, implying sensitivities to NP scales of the order of 10, 8 and 12 TeV for $\mathcal{O}_{\Phi 2}$, \mathcal{O}_{UB} and \mathcal{O}_{UW} respectively. This study is further augmented by looking at the angular distribution of $e^-e^+ \rightarrow \gamma\gamma$, which is sensitive to a different combination of the \mathcal{O}_{UB} and \mathcal{O}_{UW} couplings, implying also sensitivities to NP scales of 20 and 12 TeV .

We have then considered $\gamma\gamma$ collision processes. In boson pair production one can feel NP effects associated to scales up to $\Lambda_{NP} \simeq 20TeV$ for collider energies up to $2TeV$. This can be achieved by simply measuring final gauge boson p_T distributions. A comparison of the effects in the various final states WW , ZZ , HH , γZ and $\gamma\gamma$ including an analysis of final spin states, (i.e. separating $W_T(Z_T)$ from $W_L(Z_L)$ states), should allow a selection among the seven candidate operators.

At a linear e^+e^- collider the cross section of the process $\gamma\gamma \rightarrow H$ is the best way to study the Higgs boson, if its mass allows its production. We showed that the sensitivity limits on the NP couplings are at the 10^{-3} level, implying new physics scales up to 65 TeV , depending on the nature of the NP operator.

We have then shown that independently of the production mechanism, having at our disposal a few thousands of Higgs produced (either in $e^+e^- \rightarrow HZ$ or in $\gamma\gamma \rightarrow H$), enables the disentangling of the \mathcal{O}_{UB} and \mathcal{O}_{UW} operators by looking at the Higgs branching ratios into WW , ZZ , $\gamma\gamma$, γZ . Because these branching ratios react differently to the presence of each of these operators. This is illustrated with the ratios of these channels to the $b\bar{b}$ one which is unaffected by this kind of NP. Most spectacular for the disentangling of the various operators seem to be the ratios WW/ZZ and $\gamma\gamma/\gamma Z$. The first one, which is applicable in the intermediate and high Higgs mass range, allows to disentangle \mathcal{O}_{UB} from \mathcal{O}_{UW} down to values of the order of 10^{-1} , whereas the second one, applicable in the light Higgs case, is sensitive to couplings down to the 10^{-3} level or less.

A direct identification of CP violation requires either an analysis of the W or Z spin density matrix through their fermionic decay distributions [1], or the observation of a suitable asymmetry with linearly polarized photon beams.

Finally we emphasize that the occurrence of anomalous terms in gauge or Higgs boson couplings would be of great interest for tracing the origin of NP and its basic properties.

Acknowledgements

This work has been partially supported by the EC contract CHRX-CT94-0579.

References

- [1] G.J. Gounaris, F.M. Renard and N.D. Vlachos, Montpellier and Thessaloniki preprint PM/95-30, THES-TP 95-08, to appear in Nucl.Phys.B..
- [2] G.J. Gounaris and F.M. Renard, hep-ph/9505429 Montpellier and Thessaloniki preprint PM/95-20, THES-TP 95/07, to appear in Zeit. f. Physik.
- [3] G.J. Gounaris, J. Layssac and F.M. Renard, hep-ph/9505430 Montpellier and Thessaloniki preprint PM/95-11, THES-TP 95/06, to appear in Zeit. f. Physik.